Local volume change vs overall volume constancy during crenulation cleavage development in low grade rocks

DILIP SAHA

Geological Studies Unit, Indian Statistical Institute, 203 Barrackpore Trunk Road, Calcutta 700035, India

(*Received* 9 *October* 1996; *accepted in revised form* 29 *November* 1997)

Abstract—The role of volume change in crenulation cleavage development involving possible pressure solution of quartz and mica is investigated taking into account two end-member crenulation cleavage evolutionary models, involving (1) mica loss from microlithons and (2) immobile mica. Mathematical relationships derived for both models are used to generate data sets for comparison with measured mineralogical proportions for two samples of crenulation cleavage from the Singhbhum district, eastern India. The development of crenulation cleavage is considered to be under overall volume constancy if the average volume loss from cleavage domains is counterbalanced by average volume gain in adjoining microlithons. A test based on χ^2 statistics obtained from comparison of expected values from model calculations and observed proportions of mineral phases in microlithon and cleavage domains is proposed to accept or reject the null hypothesis of overall volume constancy during crenulation cleavage development. An application of the test to the two examples of crenulation cleavage from India suggests that mica was relatively immobile, local volume loss in cleavage domains was about 6–19%, and there was an overall volume constancy on a decimetre scale during crenulation cleavage development.

INTRODUCTION

Crenulation cleavage is a common morphological type of spaced cleavage developed in deformed rocks with an initial planar penetrative fabric, such as one developed parallel to bedding laminae in siltstones or shales or an axial planar schistosity in phyllites or quartz–mica schists (Cosgrove, 1976; Gray, 1977a; Alvarez *et al*., 1978). Various morphological types of crenulation cleavage have been distinguished on the basis of the nature of transition between cleavage domain and microlithon domain, or the relative width of the cleavage domain and microlithon domain (Gray, 1977a; Powell, 1979; Borradaile *et al*., 1982; Price and Cosgrove, 1990). Thus one may distinguish zonal crenulation cleavage in which the width of the cleavage domain is significant compared to that of the microlithon, which may contain one or more microfold hinges (Borradaile *et al*., 1982). Zonal crenulation cleavage may be discrete or gradational depending on whether the transition from cleavage domain to microlithon is sharp or gradational (Gray, 1977a,b).

Various interpretations of the morphology of zonal crenulation cleavages in natural examples of phyllites or quartz–mica schists have been put forward (Rast, 1965; Cosgrove, 1976; Marlow and Etheridge, 1977; Gray and Durney, 1979; Granath, 1980). Extant models of crenulation cleavage development suggest a redistribution of mineral phases by dissolution of quartz from cleavage domains and reprecipitation in microlithons with or without significant contribution from metamorphic reactions. The majority of published works agree that the process involves microfolding of an initial fabric and then a redistribution of mineral phases between hinge and limb to account for crenulation cleavage development. The main points of disagreement are on (a) the actual process of material redistribution, and (b) the relative contribution of metamorphic reactions in adding new mica (phyllosilicate) to the cleavage domain. The process of material redistribution may involve diffusion in a static grain boundary fluid (or a dispersed phase, e.g. Elliott, 1973; Rutter, 1983), or solution-reprecipitation (advection) under the influence of a mobile fluid phase (e.g. Granath, 1980; Etheridge *et al*., 1984; Caron *et al*., 1987).

Some work on cleavage formation (not necessarily crenulation cleavage *sensu stricto*) has considered open vs closed system behaviour as inferred from major, trace, and stable isotope chemistry (e.g. Wintsch *et al*., 1991). Under low grade metamorphic conditions metamorphic reactions are considered to be less effective in adding significant volume of new mica to the cleavage domain (Gray and Durney, 1979; Weber, 1981). Even if the dominant process of cleavage differentiation is by mineral redistribution by diffusion or advection, whether the overall volume remains constant during cleavage development has been debated (Mancktelow, 1994).

Another factor that has been emphasized is the role of chemical reactions in enhancing pressure solution ('incongruent' pressure solution of Beach, 1979; also Knipe, 1981; Rutter, 1983). In polymineralic rocks the redistribution of minerals by diffusion may not be accomplished simply by solution and diffusion of a mineral phase from source to sink. The diffusion of components of a phase will not be driven only by normal stress-induced chemical potential gradient, but may be enhanced through the free energy change accompanying the reactions at source or sink (Rutter, 1983).

Rutter argues that the precipitation of quartz in the hinge region of crenulations should not be regarded as simply representing volume for volume reprecipitation of quartz diffused from highly stressed microfold limbs, but perhaps it is only one of the products of reaction leading to mineral growth taking place at the microfold hinge region. The role of chemical transformations in mineral redistribution accompanying natural crenulation cleavage development can be systematically explored through observations under an electron microscope equipped with analytical facilities (Knipe and White, 1977; Knipe, 1981).

The scope of the present work is restricted to situations in which the growth of metamorphic mica (or other phyllosilicate) is very limited during the crenulation of a pre-existing schistose fabric or a homogeneous multilayer fabric consisting essentially of two mineral phases, for example, quartz and muscovite. The analysed data are obtained through optical microscopic observations on samples of crenulation cleavage in which optically identifiable mineral phases are the same in microlithon, cleavage domain and protolith (uncrenulated parts).

In this paper two end-member models of material redistribution are considered—(1) *Mobile mica model* (after Cosgrove, 1976) and (2) *Conservative mica model* (after Gray and Durney, 1979).

Mobile mica model

According to Cosgrove (1976) crenulation cleavage is non-pervasive, forming in finely laminated rocks and mineral fabrics as a result of microbuckling, together with some pressure solution and mineral redistribution. The intimate association of microfolding and mineral redistribution has been explained in terms of mineral migration in response to stress gradients that are established during microfolding. As folding proceeds beyond a certain degree of limb rotation (fig. 12c of Cosgrove, 1976) in a homogeneous quartz–muscovite (henceforth referred to as mica) schist fabric, the quartz grains in the limb are subjected to a larger stress, as they are no longer 'protected' by the mica framework. Because the micas in the hinge areas have not rotated much, the quartz in the hinge areas is still protected. It follows then that quartz in the limb is subjected to higher stress compared to quartz in the hinge. The stress gradient drives migration of quartz from limbs to hinge by dissolution and reprecipitation. The micas in the hinge support most of the compression and are under a relatively larger compressive stress compared to mica in the limbs. Pressure solution of mica will therefore tend to occur more readily in the hinge areas and there will be a tendency for it to migrate from hinge areas towards the limbs. The cleavage domains follow the limbs and there will be a consequent relative concentration of mica in these domains. Since there is redistribution of mica in addition to quartz, the above model is referred to as the *mobile mica model*.

Conservative mica model

According to Gray and Durney (1979) microfolding, generally internal buckling, and solution–deposition processes, in that order, are necessary for crenulation cleavage development. More soluble mineral phases (say quartz in a quartz–mica fabric) are dissolved from along the limbs and transferred to fold hinges, where they are deposited, presumably as overgrowths on existing grains/layers. The diffusive flux is in the direction of normal stress decrease; that is from areas of high chemical potential, fold limbs, to areas of low potential, fold hinges. Based on petrographic observations, a series of mineral mobility for low grade metamorphic rocks has been suggested for which quartz is more mobile than mica and chlorite (Heald, 1955; Trurnit, 1968; Gray and Durney, 1979). As a result micas may become part of the solution residue of a pressure solution zone along the fold limb and micas in fold hinges, areas of low chemical potential, are not affected by diffusion.

In either model the diffusion path with respect to a mineral component is fundamentally restricted. Therefore, in both cases, the deformation and attendant cleavage development is volume conservative on a decimeter scale taking into account a few fold hinges and adjacent limbs. The overall volume constancy refers to this scale only. Given the above end-member models of mineral redistribution, and further assuming that little new mica is added into the crenulated fabric by metamorphic reaction during or post-dating crenulation cleavage development, it is shown here that a test can be devised to examine whether crenulation cleavage development in a quartz–mica schist fabric or multilayer fabric takes place under overall volume constancy. The exercise also provides an estimate of local volume changes (dilatation) in microlithon and cleavage domains for naturally occurring crenulation cleavage.

The chemical potential gradient, which acts as the driving force behind pressure solution during crenulation cleavage development, is controlled by the limb dip of the growing microfolds (Gray and Durney, 1979). Other factors such as grain size, chemical reaction and the thickness of intergranular fluid film may also control the strain rate due to pressure solution (e.g. Durney, 1972; Rutter, 1976, 1983; Beach, 1979). However, the role of these factors are not taken into account in the present analysis.

THEORETICAL BASIS OF THE TEST OF OVERALL VOLUME CONSTANCY

According to the models discussed above, the development of crenulation cleavage involves local volume

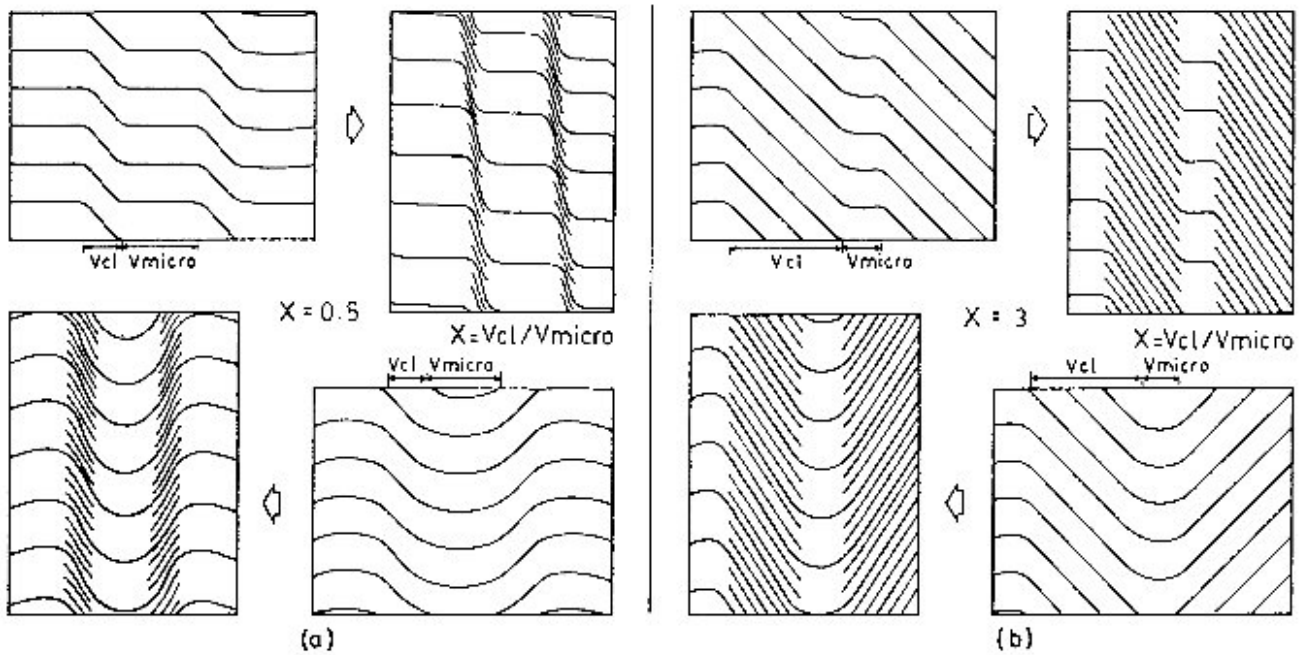

Fig. 1. Fold style factor (X) and final cleavage domain (hachured) appearance for zonal crenulation cleavage. The diagrams show cleavage development at 25% E–W shortening for two different X values under plane strain, constant volume deformation and cleavage differentiation. The upper panel shows asymmetric folds; the lower panel symmetric folds. Note that the limb dip is more important than asymmetry of the folds. (a) $X = 0.5$. (b) $X = 3$.

loss in a cleavage domain which, depending on fold style, may follow both or alternate limbs of microfolds (Hobbs *et al.*, 1976), compared to the adjoining microlithon (Fig. 1). For example, the lower panel in Fig. 1 shows fold limbs symmetric with respect to maximum compression direction, assumed to be east–west here. The resultant cleavage domains follow both fold limbs. Fold limbs on the upper panel in Fig. 1, on the other hand, are asymmetric with respect to the maximum compression direction. The resultant cleavage domain follows the limb making a larger angle with the maximum compression direction, while the other limb is preserved in the microlithon.

Mathematical derivation of relationships in mobile mica model

It is assumed that a % of quartz is lost from the cleavage domains on average and that b % of mica is removed from the microlithons on average. As the original fabric is assumed to be homogeneous across the primary lamination or schistosity, $Q + M = 100$ in the precursors to either the microlithon or the cleavage domains, where Q and M represent the percentages of quartz and mica, respectively, in the original (protolith) fabric. However, we start with 100 volume units of the microlithon domain as opposed to $100.X$ volume units of the cleavage domain, as X may have a value other than unity depending on fold style. X is defined as the pre-differentiation volume ratio of cleavage domain to microlithon (Fig. 1).

Where the folded fabric is symmetrically disposed with respect to the maximum compression direction and where the hinge region is wide compared to the limb with appreciable dip, X will be less than unity (Fig. 1a). For microfolds with sharp hinges and relatively long limbs X will be greater than unity. Where the folded fabric is asymmetric with respect to the maximum compression direction, depending on the exact geometry of the fold, X may represent the volume ratio of the two limbs (Fig. 1b). Let us consider the changes due to pressure solution differentiation in quartz and mica volumes separately for microlithon and cleavage domains.

Microlithon domain

The local quartz volume gain = $aQX/100$. The local mica volume loss = $bM/100$. The post-differentiation volume of microlithon is given by the left hand side in

$$(1 + aX/100)Q + (1 - b/100)M = 100 + FX, \quad (1)$$

where F is the net change (loss) in volume in 100 volume units of cleavage domains.

Cleavage domain

The local quartz volume loss = $aQX/100$. The local mica volume gain = $bM/100$. The post-differentiation volume of the cleavage domain is obtained by the left hand side in:

$$(1 - a/100)Q + (1 + b/100X)M = 100 - F. \quad (2)$$

Subtracting equation (2) from equation (1),

$$F = (aQ - bM/X)/100. \quad (3)$$

Rearranging equation (3)

$$bM/X = aQ - 100F. \quad (3a)$$

Since, $b \geq 0$, $M > 0$ and $X > 0$, for a given X, F will be maximized if the first term on the right hand side of equation (3a) is maximized for a given X. For a given original fabric Q is fixed and the upper limit of a is 100. Therefore, the maximum F value, $(F)_{max}$ is given by

$$(F)_{max} = Q. \quad (4)$$

Again the minimum value of a (denoted by a_{min}) is obtained from equation (3a),

$$a_{min} = 100F/Q. \quad (4a)$$

For given $F = F_i$, say, a specific value of F for theoretical calculations,

$$b = X(aQ - 100\,F_i)/M \quad (5)$$

$$\text{For } X = 1,\ b = (aQ - 100\,F_i)/M. \quad (6)$$

In the *mobile mica model* the set of equations (1) and (3a) or (5) lead us to a situation in which only Q and M (quartz and mica percentages in the uncrenulated fabric) are known, a and b are unknown and so are F and X. For calculation of the expected quartz and mica proportions in the crenulated and differentiated fabric, X is given a pre-set value for a particular run. One can compute the minimum of a from equation (4a) and the corresponding b from equation (3a) if F is also known. From the previous argument, a varies in the range, $a_{min} < a < 100$, and computations are done for F values in the range $1 < F \leq Q$. For given F and X, and corresponding a and b, the expected quartz and mica proportions in the microlithon domain are then obtained by calculating:

$$(1+aX/100)Q/[(1+aX/100)Q+(1-b/100)M]$$

for quartz and

$$(1-b/100)M/[(1+aX/100)Q+(1-b/100)M]$$

for mica. The expected quartz and mica proportions in the cleavage domain are similarly obtained by considering the left hand side of equation (2).

Mathematical derivation of relations in conservative mica model

Gray and Durney (1979) considered that the dissolution and diffusion of mica during crenulation cleavage development is insignificant and that the differentiation is effected solely by the removal of quartz from prospective cleavage domains (say microfold limbs) and its diffusion to and precipitation in the prospective microlithon domain (say microfold hinges). Accordingly, only a % quartz is removed from the cleavage domain and the mathematical relations are simplified as given below.

Microlithon domain

The local quartz volume gain = $aQX/100$, and mica remains immobile. The post-differentiation volume of the microlithon domain is given by the left hand side in

$$(1 + aX/100)Q + M = 100 + FX. \quad (7)$$

Cleavage domain

The post-differentiation volume of the cleavage domains is given by the left hand side in:

$$(1 - a/100)Q + M = 100 - F, \quad (8)$$

where a, Q, M, F and X have their meaning as indicated earlier for the mobile mica model. Eliminating M and X from equations (7) and (8) we get

$$F = aQ/100. \quad (9)$$

Note that equation (9) can be derived from equation (3) by putting $b = 0$.

By setting the X value first and then F in the range $1 < F \leq Q$, one can calculate a from equation (9). The expected quartz and mica proportions in the microlithon domain would be given by the expressions $(1 + aX/100)Q/[(1 + aX/100)Q + M]$ and $M/[(1 + aX/100)Q + M]$, respectively. Similarly, for the cleavage domain the expected quartz and mica proportions would be given by the expressions $(1 - a/100)Q/[(1 - a/100)Q + M]$ and $M/[(1 - a/100) \times Q + M]$, respectively.

The test

From the above, the expected final proportions of quartz and mica in the cleavage and microlithon domains can be calculated in either of the two end member models. The test compares these expected values with the observed proportions of quartz and mica in the differentiated fabric for a natural example of crenulation cleavage. The proportions of quartz and mica in natural crenulated fabrics can be obtained by routine petrographic analysis of a thin section by optical microscopy using a Swift automatic point counter (Galehouse, 1971). The crux of the problem in the above comparison lies in what is to be considered a significant difference between observed and expected values. A chi-square test is applied here as follows. A (2×2) contingency table is prepared, where each cell represents the observed proportion (expressed as %) of quartz or mica in the cleavage domain or microlithon domain (Table 1).

Table 1. A (2 × 2) contingency table showing proportions of quartz and mica (bold entries) in cleavage (**l**) and microlithon (**h**) domains

	Quartz	Mica	Total
Cleavage domain	**Q(l)**	**M(l)**	100
Microlithon domain	**Q(h)**	**M(h)**	100
			200

The chi-square statistic (χ^2) is calculated from $\chi^2=(\Sigma\ (O_i-E_i)^2/E_i)$ (Cheeney, 1983), where O_i is the observed value, E_i is the expected value corresponding to each cell in the (2 × 2) contingency table, N is the sample size (=200 here). For given F and X values χ^2 is calculated for the permitted range of a values. The null hypothesis is taken as: crenulation cleavage development occurs under overall volume constancy. For any natural example of crenulation cleavage differentiation by mineral redistribution the χ^2 statistic can be computed for the range $0 < F < (F)_{max}$ for the mobile mica model or the conservative mica model. A critical region (significance level) of $\alpha = 0.05$ is selected and corresponding critical value of χ^2 is obtained from a table of theoretical distribution (Berenson *et al.*, 1983). The degree of freedom in the above case is 2 (No. of cells − No. of independent constraints). By plotting χ^2 values against a values and drawing the cut-off line corresponding to $\alpha = 0.05$, one can find out which combinations of a, b and F are permissible under the null hypothesis of overall volume constancy. The null hypothesis is rejected only if the chi-square statistic is greater than the critical value of χ^2 for a given significance level; that is the deviation of the observed value from the expected cannot be explained by sampling error. The alternative is to consider some degree of overall volume change.

AN APPLICATION OF THE TEST

Sample description

The above test of overall volume constancy during crenulation cleavage development has been applied on two natural examples of crenulation cleavage in mica-schist (Fig. 2). The mica-schist specimen (No. 91-04) collected from Galudih, Singbhum district, eastern India belongs to the Chaibasa Formation (Dunn and Dey, 1942; Sarkar and Saha, 1977; Saha, 1995). The hand specimen is from a garnet-bearing schist; however, microfolding of the schistosity is a later event when the garnets were partly replaced by chlorite ($D3$ of Sarkar, 1982). Another crenulated phyllite specimen (No. 22N-1) collected from Rohinbera, Singhbhum district, eastern India belongs to the lower part of the Dhanjori Group (Dunn and Dey, 1942; Sarkar and Saha, 1977). In both examples uncrenulated schists can be physically traced to domains where the earlier schistosity is crenulated with development of a crenulation cleavage (Fig. 2). For the purpose of obtaining modal composition thin sections were prepared from both uncrenulated and crenulated domains in either of the examples. The essential textural and microstructral features of the specimens are given below.

Texture and microstructure in the Galudih sample (No. 91-04). Optical microscopic observation of the protolith (uncrenulated domain) shows a homogeneous quartz–muscovite schist fabric (average quartz grain size about 90 μm, Fig. 3) with minor chlorite, garnet and opaques. In the crenulated domains the schist fabric is affected by microfolds with wavelengths of 5–6 mm (6–7 pairs of hinges over 3 cm of the thin section, Fig. 3a). Cleavage domains are defined by the relative concentration of muscovite and alignment of muscovite cleavage lamellae at a smaller angle to the microfold axial trace (Fig. 3f). These domains apparently follow microfold limbs of higher dip. Recrystallized muscovite grains are few and far between. Well-developed cleavage seams are characterized by quartz grains of larger aspect ratio (Fig. 4), truncation of quartz grain boundaries and some unusually slender grains (Fig. 3g). The features are indicative of removal of quartz by pressure solution from the cleavage domains.

On the other hands the microlithon domains are marked by lower aspect ratios of the quartz grains (Fig. 3f). Muscovites are bent and quartz grains show undulose extinction over microfold hinges, but they are not recrystallized. Although overgrowths on microlithon quartz grains are not apparent from direct optical microscopy, a comparison of the mean size and shape of quartz grains from the microlithon and cleavage domains, respectively (Fig. 4), shows that while the aspect ratio of quartz grains in the cleavage domain increases the average size decreases relative to

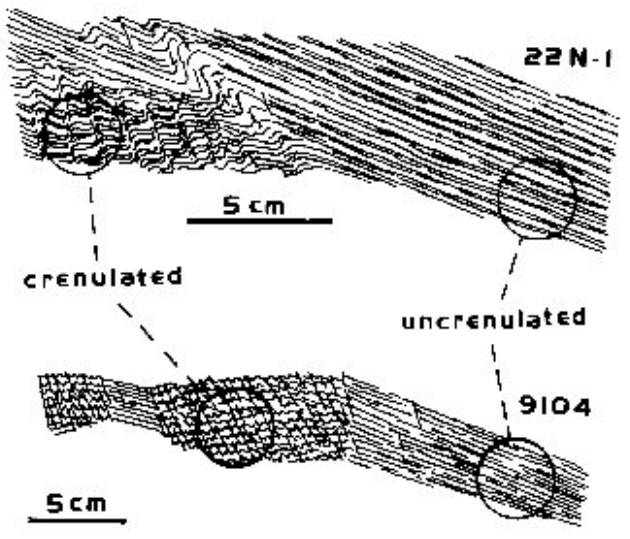

Fig. 2. Relationship between protolith (uncrenulated) and crenulated domains in two samples of crenulation cleavage from the Singhbhum district, eastern India. Specimen No. 91-04 is from Galudih and specimen No. 22N-1 from Rohinbera. The positions of thin sections cut from the different domains are marked with circles.

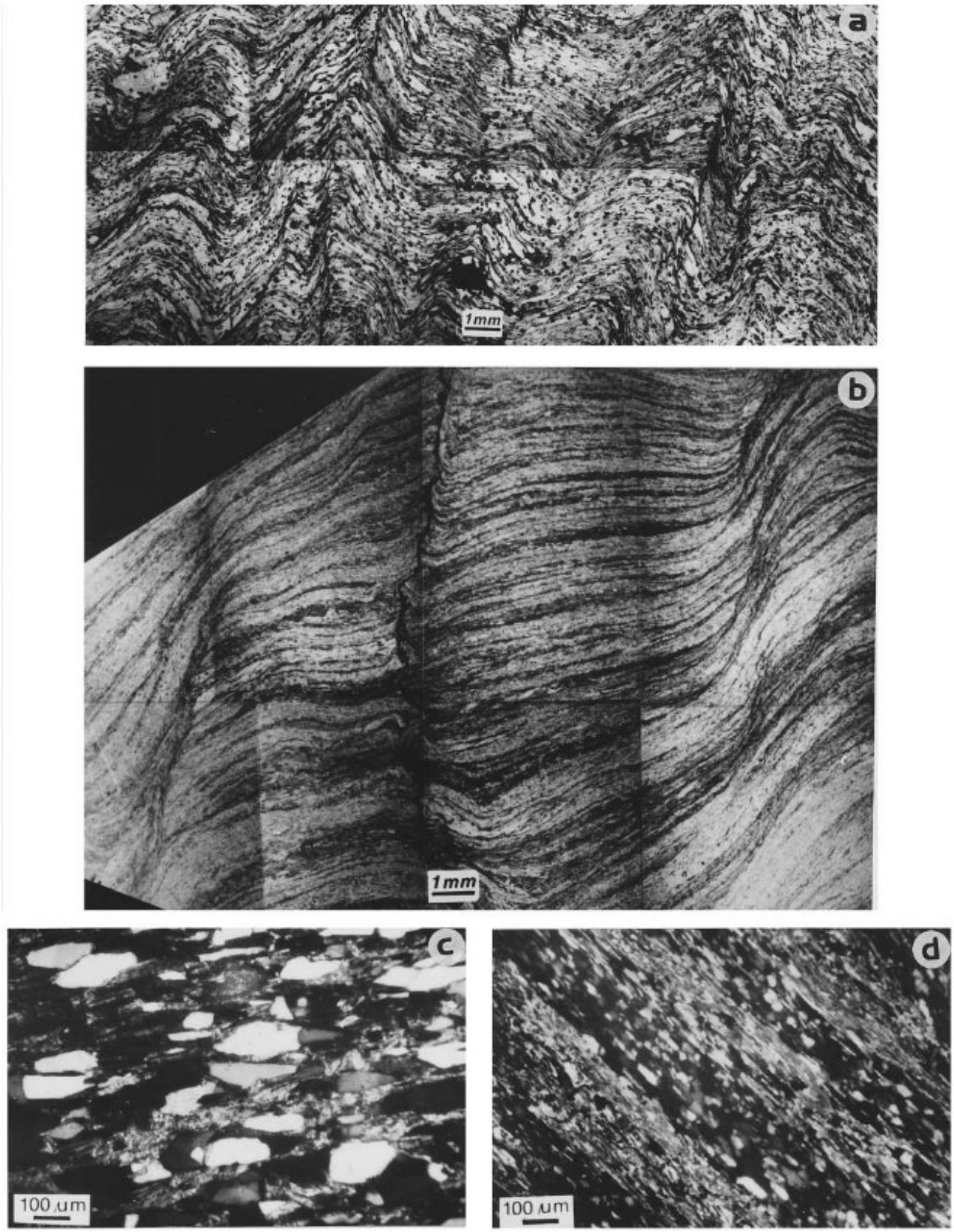

Fig. 3(a–d)

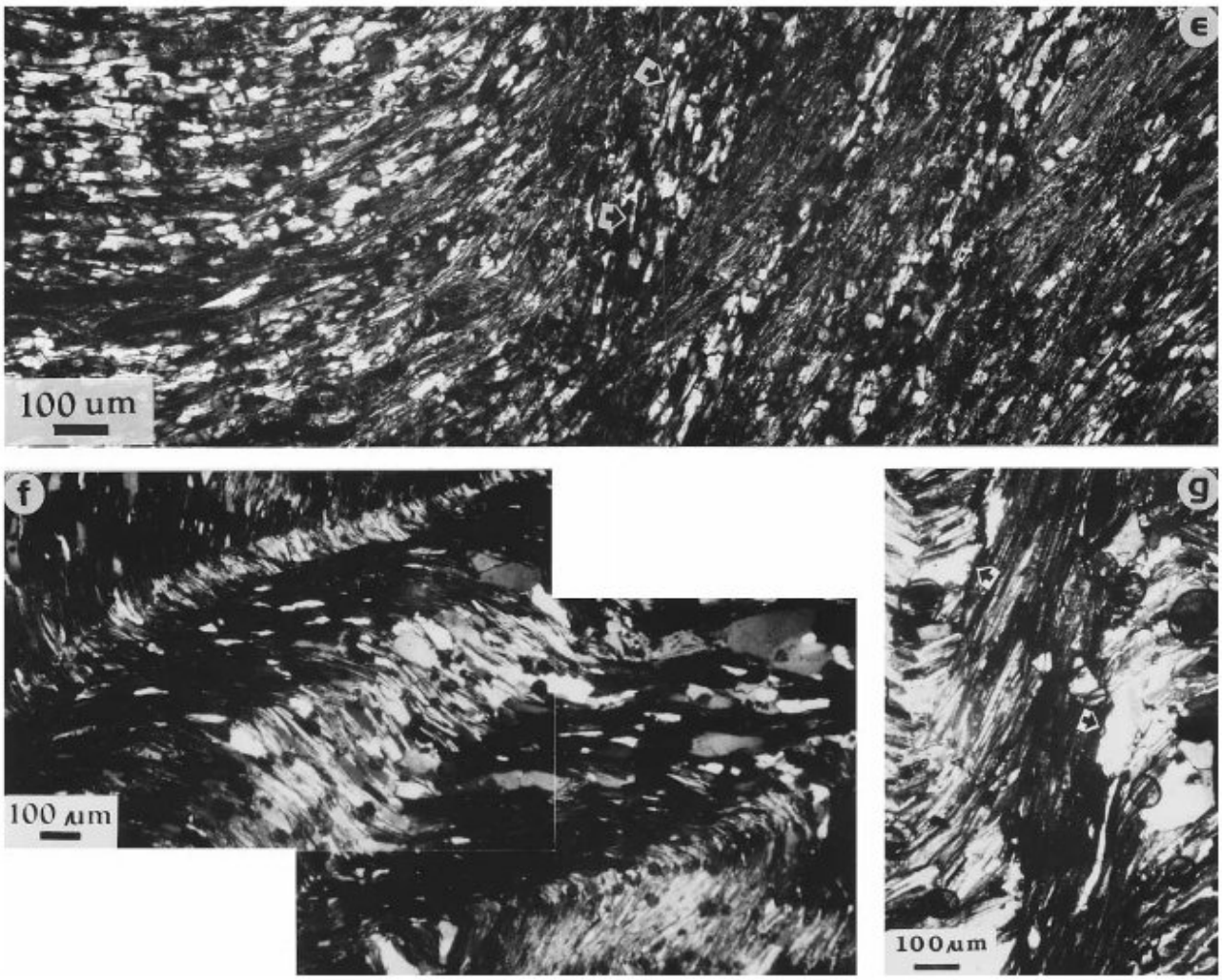

Fig. 3. Gross morphology of discrete to gradational types of zonal crenulation cleavage, protolith fabric and pressure solution microstructures in the studied rocks. (a) Slightly asymmetric to symmetric crenulations; cleavage domains follow one or other limb; specimen No. 91-04, Galudih. (b) Cleavage domains follow the steeper limb of asymmetric folds, specimen No. 22N-1, Rohinbera. (c) Homogeneous quartz–mica schist fabric in the protolith of the Galudih sample. (d) Fine multilayer fabric in the protolith of the Rohinbera sample; note the schistose fabric internal to both quartz-rich and muscovite-rich layers. (e) Photomosaic showing change in quartz grain aspect ratio from microlithon (left half of photograph) to cleavage domain (right); some slender quartz grains in the cleavage domain are marked by arrows; Rohinbera example; detail from the right-most cleavage seam in (b). (f) Higher aspect ratio of quartz grains in the cleavage domain, Galudih example. Note the strong alignment of mica indicated by simultaneous extinction along NE–SW strips on the photomosaic. (g) Truncated margins of quartz (arrows) along a cleavage domain boundary and unusually thin quartz grains without any subgrain formation within the cleavage domain (bottom centre of photograph); Galudih example.

the corresponding parameters in the protolith; the average grain size of quartz is higher (Fig. 4c) and the aspect ratio is lower in the microlithon than in the protolith (Fig. 4a). The observations are suggestive of selective dissolution of quartz from cleavage domains and reprecipitation in the adjoining microlithons.

Texture and microstructure in the Rohinbera sample (No. 22N-1). The protolith (uncrenulated domain) shows a fine multilayer fabric with alternate layers relatively rich in quartz or muscovite (average quartz grain size ~30 μm, Fig. 3d). The layers are 150–200 (μm thick. Internally, either layer has a type of schistose fabric marked by alignment of muscovite cleavage lamellae and long axes of quartz and muscovite grains statistically parallel to compositional layering (Fig. 3d). In the crenulated part the multilayer shows a number of asymmetric folds (wavelengths of the order of a centimetre), with cleavage seams following the relatively steeper limb (Fig. 3b).

On average quartz shows a relatively higher aspect ratio but lower grain size in the cleavage domains compared to the protolith (Figs 3e & 4b & d). On the other hand, quartz has a relatively lower aspect ratio but higher average grain size in the microlithon domains compared to corresponding parameters in the protolith (Fig. 4b & d). Although some quartz-rich layers can be traced across cleavage domains to the microlithons on either side, the layers are definitely attenuated in the cleavage domain; some other quartz-rich layers are truncated at the cleavage domain

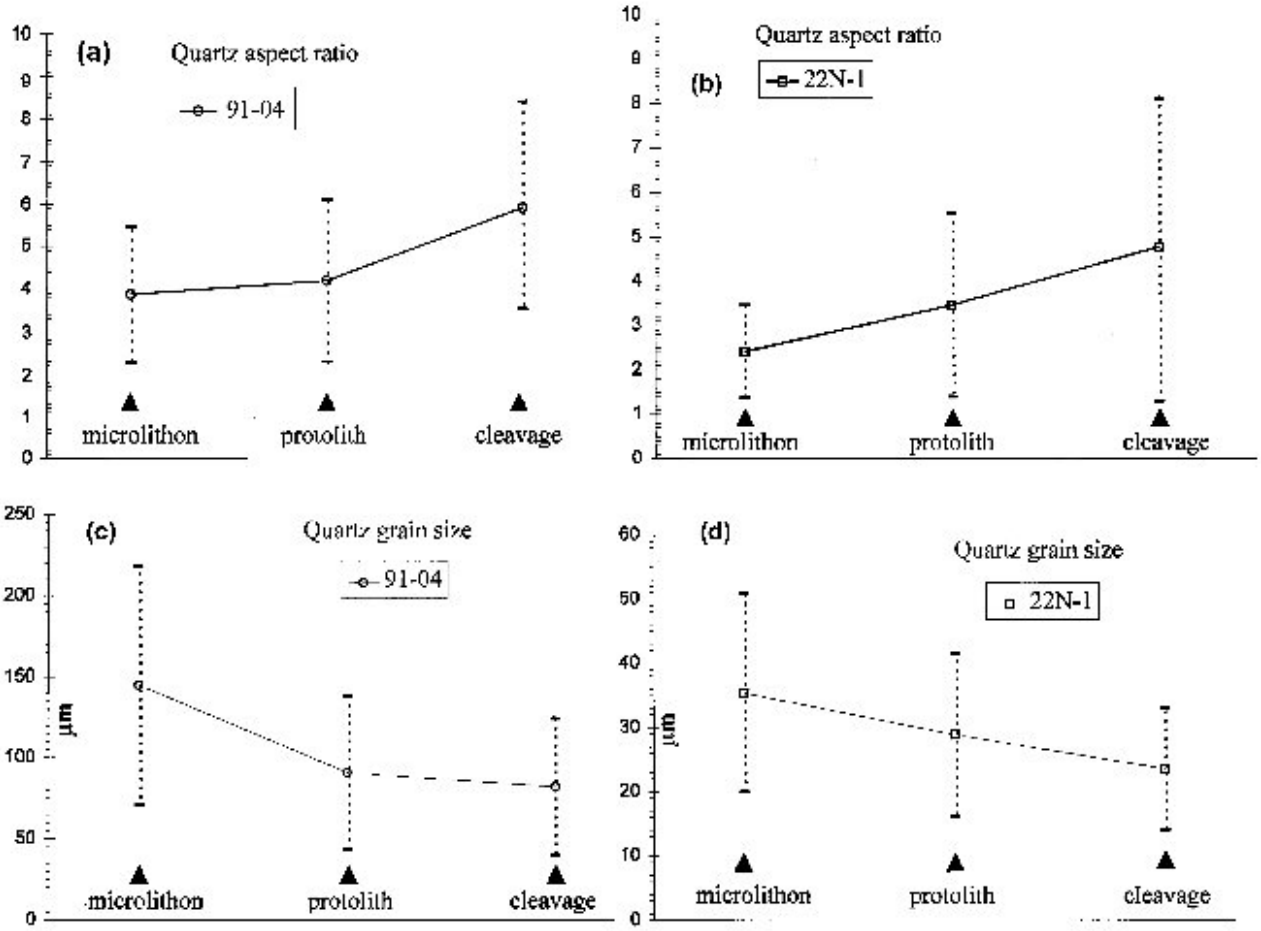

Fig. 4. Modification of quartz aspect ratio (a & b) and grain size (c & d) due to solution transfer in the Galudih and Rohinbera samples. $1/n\Sigma(d_{i1}d_{i2})^{1/2}$ is taken as the average grain size, where d_{i1} and d_{i2} represent mutually perpendicular longest and shortest intercepts through a grain centre. Similarly, $1/n\Sigma(d_{i1}/d_{i2})$ gives the average aspect ratio. n = 40, 55 and 43, respectively, in microlithon, protolith and cleavage domains in (a & c); corresponding figures for (b & d) are 31, 50 and 31.

boundary (Fig. 3b). The above features are again indicative of removal by pressure solution of quartz from cleavage domains and reprecipitation in the microlithon domains. Evidently the above examples represent crenulation cleavage development under low grade metamorphic conditions, under which mineral redistribution by pressure solution–diffusion–precipitation is most effective in cleavage differentiation (Gray and Durney, 1979).

Modal composition

Optical microscopic observations on thin sections from the above specimens indicate that the dominant mineral phases are muscovite and quartz with minor amounts of chlorite and a few garnet porphyroblasts (specimen No. 91-04 only). Garnet, which apparently formed earlier than the microfolds, is deliberately excluded from the point counting while chlorite is clubbed together with mica. The overall proportion of quartz to mica in the original fabric (uncrenulated parts in Fig. 2) from which the crenulated fabric is produced, is estimated from modal counts with a Swift Automatic Point Counter. About 2500 counts were made for the Galudih sample, which has a coarse schistose fabric and 4000 counts for the Rohinbera sample, having a finer but multilayered fabric. Counts were made at steps of one-sixth of a millimetre on parallel line traverses on thin sections prepared from uncrenulated parts of the rocks (Table 2). The morphology of the cleavage in both examples varies from discrete to gradational types of zonal crenulation cleavage (Gray, 1977a,b; Powell, 1979; Borradaile *et al*., 1982) (Fig. 3). The percentages of mineral phases in the microlithon and cleavage domains are estimated by restricting the traverses to individual domains within a thin section cut from the crenulated parts (about 1400 counts for the cleavage domain and 4700 counts for the microlithon domain in specimen 22N-1; and in specimen 91-04 1000 and 1200 counts, respectively).

Using the algebra detailed above, the expected quartz and mica proportions in the cleavage and microlithon domains for the above specimens were

Table 2. Modal composition in different domains of the crenulation cleavage fabric and original rock in the examples studied. Plus–minus figures represent 95% confidence limits (Kelley, 1971)

Specimen No.	Mineral phase	Modal composition		
		Protolith	Cleavage domain	Microlithon domain
91-04	quartz	28.85 ± 1.80	24.40 ± 2.67	36.50 ± 2.75
	mica	71.15 ± 1.80	75.60 ± 2.67	63.50 ± 2.75
22N-1	quartz	57.89 ± 1.54	48.20 ± 2.63	66.20 ± 1.34
	mica	42.11 ± 1.54	51.80 ± 2.63	33.80 ± 1.34

computed for various values of F and a (and b) in the range $0 < F < F_{max}$. The expected values were then compared with the actual estimates from modal analysis. (A Fortran coding for the above calculation adaptable to an IBM compatible PC has been written and is available on request.)

Results

Galudih example. Starting with the data in Table 2, computations were done as outlined earlier first for the mobile mica model. The test is applied by plotting $\ln(\chi^2)$ against a, the percentage quartz lost from cleavage domain under given local volume change F % in the cleavage domain (Fig. 5). The significance level is set at $\alpha = 0.05$. (There is 5% chance χ^2 would have values larger than the cut-off value $\chi^2_{2,0.05} = 5.99$, Berensen *et al.*, 1983.) A set of F, a, b will be in accord with the null hypothesis of overall volume constancy only if the calculated χ^2 statistic is less than or equal to the cut-off value. The range of F and corresponding a and b values for which volume constancy is acceptable are shown in Table 3. In this case $>15\%$ local volume change in the cleavage domain ($F > 15$) is incompatible with overall volume constancy when fold style factor, X, equals 1. The minimum of all computed χ^2 values ($\ln \chi^2 = -1.296$, Table 3) in the range $1 < F \leq 15$ and for $X = 1$ represents a case in which the expected quartz and mica proportions obtained by the model calculations for the different domains of the crenulated fabric are very close to those observed; the corresponding F–a–b combination is referred to as 'optimum' for a given X. By varying X in the range 0.1 (that is, very wide hinge region compared to limbs) to 10 (that is, long limbs, narrow hinge), one can find the smallest of all χ^2 corresponding to the 'optimum' F–a–b combination in each case. Table 3 shows that at $X = 2$, $F = 6\%$, $a = 20.8\%$ and $b = 0$ (zero mobility of mica), $\ln \chi^2 = -7.63$, referred to here as a global minimum for the Galudih example. Therefore, it is concluded that even under the mobile mica model, $b = 0$ provides, statistically speaking, the best estimate of local volume change ($F \sim 6\%$) compatible with overall volume constancy during crenulation cleavage development. The test shows that volume constancy can be accepted within the limits of error. Similarly, computations following the conservative mica model of crenulation cleavage development show that the global minimum of $\ln(\chi^2)$ is obtained at $X = 2$, $F = 6\%$ and $a = 20.8\%$ (Table 4). Evidently there is convergence of results from the two end-member model calculations.

Rohinbera example. The first set of computations following the mobile mica model shows that overall volume constancy during crenulation cleavage development is acceptable for local volume changes up to 33% of cleavage domain ($F \leq 33$, Table 3) at a significance level of $\alpha = 0.05$. The global minimum of χ^2 ($\ln \chi^2 \sim -6.53$) is attained when $X = 1.3$, $F = 19\%$, $a = 32.82\%$ and $b = 0$. Results from the test show that the best estimate of local volume change under overall volume constancy in the Rohinbera example is 19% in the cleavage domain. Computations following the conservative mica model lead to similar values of

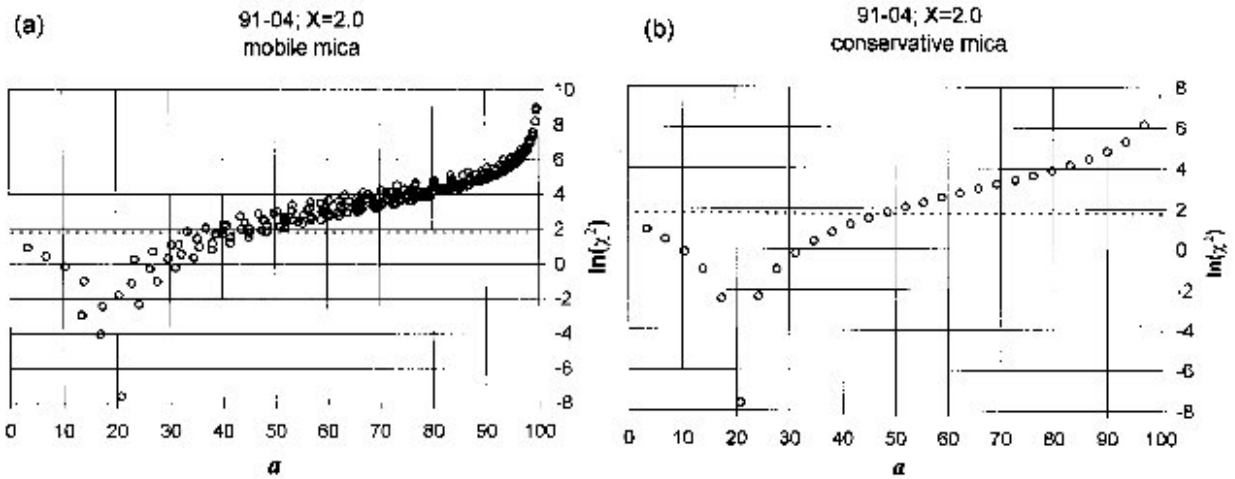

Fig. 5. Results from the chi-square test for overall volume constancy during crenulation cleavage development in the Galudih example. The test has 95% significance level ($\alpha = 0.05$, $\chi^2_{2,\alpha} = 5.99$). In each a–ln (χ^2) plot the dashed horizontal line corresponding to $\alpha = 0.05$ marks the cut off line (ln (χ^2) = 1.79) below which overall volume constancy is accepted. See text and Tables 3 and 4 for details. (a) Fold style factor (X) = 2; mobile mica model. (b) $X = 2.0$; conservative mica model. Overall volume constancy is accepted up to a local volume change of $F = 15$, irrespective of the model.

Table 3. F domain and a and b values over which volume constancy is accepted for crenulation cleavage development for the mobile mica model in the Indian examples at the 95% significance level ($\alpha = 0.05$, $\chi_{2,\alpha} = 5.99$). Minimum divergence between observed and expected quartz–mica proportions is observed at the 'optimum' ln (χ^2)–F–a–b combination. *Maximum permissible a value at given F and corresponding b value

Specimen No.	X	Volume constancy accepted	ln (χ^2)	Optimum			Upper F*	
				F	a	b	a	b
91-04	0.1	$F \leq 14$	0.910	01	18.47	0.61	48.53	0.00
	0.25	$F \leq 14$	0.660	01	20.47	1.72	48.53	0.00
	0.5	$F \leq 15$	0.137	01	22.47	3.85	51.99	0.00
	1.0	$F \leq 15$	−1.296	01	21.47	7.30	51.99	0.00
	2.0	$F \leq 13$	−7.630	06	20.80	0.00	45.06	0.00
	5.0	$F \leq 07$	−0.992	03	07.93	2.03	24.26	0.00
	10.0	$F \leq 03$	−0.390	01	04.47	4.05	10.40	0.00
22N-1	0.1	$F \leq 31$	0.793	01	18.73	2.34	53.55	0.00
	0.25	$F \leq 32$	0.322	01	19.73	6.19	55.28	0.00
	0.5	$F \leq 33$	−0.844	01	19.73	12.37	57.00	0.00
	1.0	$F \leq 33$	−6.359	09	24.55	12.37	57.00	0.00
	1.3	$F \leq 32$	−6.534	19	32.82	0.00	55.28	0.00
	2.5	$F \leq 27$	−0.449	14	24.18	0.00	46.64	0.00
	5.0	$F \leq 15$	0.709	07	12.09	0.00	25.91	0.00
	10.0	$F \leq 06$	1.083	03	05.18	0.00	10.36	0.00

F, a and b (compare Tables 3 and 4). The null hypothesis of overall volume constancy is acceptable within limits of error for the Rohinbera example and there is convergence of results from computations following the two models (Figs 5 and 7).

Influence of fold style factor, X

As defined earlier the fold style factor, X, is the initial volume ratio of cleavage domain and microlithon domain (Fig. 1). In particular, symmetric angular folds have a narrow hinge domain compared to the limb domain and accordingly have X values well in excess of 1, whereas folds with rounded hinges and narrow limb domain or those with gross asymmetry have X less than 1 (Fig. 1). For a particular natural example of differentiated cleavage it is difficult to determine the exact value of X. However, one can only attempt to bracket X, knowing the final overall volume ratio of cleavage domains and assuming overall volume constancy. Computations show that for X values at least an order of magnitude higher or lower than 1, there is a significant change in the bounds of F under which volume constancy is acceptable (Tables 3 and 4). Relatively larger values of X ($\geq$37 for Galudih and $\geq$58 for Rohinbera) lead to the rejection of the null hypothesis at a significance level of $\alpha = 0.05$.

Note also that in the Rohinbera sample the lowest of the optimum ln (χ^2) values (referred to here as global minimum) is associated with $X = 1.3$ (Fig. 6), i.e. the cleavage domain was apparently 1.3 times as wide as the microlithon to start with. The corresponding global minimum ln (χ^2) value in the Galudih example is obtained when $X = 2$ (Fig. 5), i.e. the microlithon was half as wide as the cleavage domain to start with. These minimum ln (χ^2) values, −6.53 (Rohinbera) and −7.63 (Galudih), are associated with a very stringent significance limit, $\alpha \geq 0.99$, and, therefore, are con-

Table 4. F domain and a values over which volume constancy is accepted for crenulation cleavage development for the conservative mica model in the examples cited at the 95% significance level ($\alpha = 0.05$, $\chi_{2,\alpha} = 5.99$). Minimum divergence between observed and expected quartz–mica proportions is obtained at the 'optimum' ln (χ^2)–F–a combination. *Maximum permissible a value at given F

Specimen No.	X	Volume constancy accepted	ln (χ^2)	Optimum		Upper F*
				F	a	a
91-04	0.1	$F \leq 14$	0.922	07	24.26	48.53
	0.25	$F \leq 14$	0.698	07	24.26	48.53
	0.5	$F \leq 15$	0.254	08	27.73	51.99
	1.0	$F \leq 15$	−0.858	08	27.73	51.99
	2.0	$F \leq 13$	−7.630	06	20.80	45.06
	5.0	$F \leq 07$	−0.990	03	10.40	24.26
	10.0	$F \leq 03$	−0.288	01	03.47	10.40
22N-1	0.1	$F \leq 31$	0.85	19	32.82	53.55
	0.25	$F \leq 32$	0.52	20	34.55	55.28
	0.5	$F \leq 33$	−0.13	21	36.28	57.00
	1.0	$F \leq 33$	−2.29	20	34.55	57.00
	1.3	$F \leq 32$	−6.53	19	32.82	55.28
	2.5	$F \leq 27$	−0.45	14	24.18	46.64
	5.0	$F \leq 15$	0.31	07	12.09	25.91
	10.0	$F \leq 06$	1.08	03	05.18	10.36

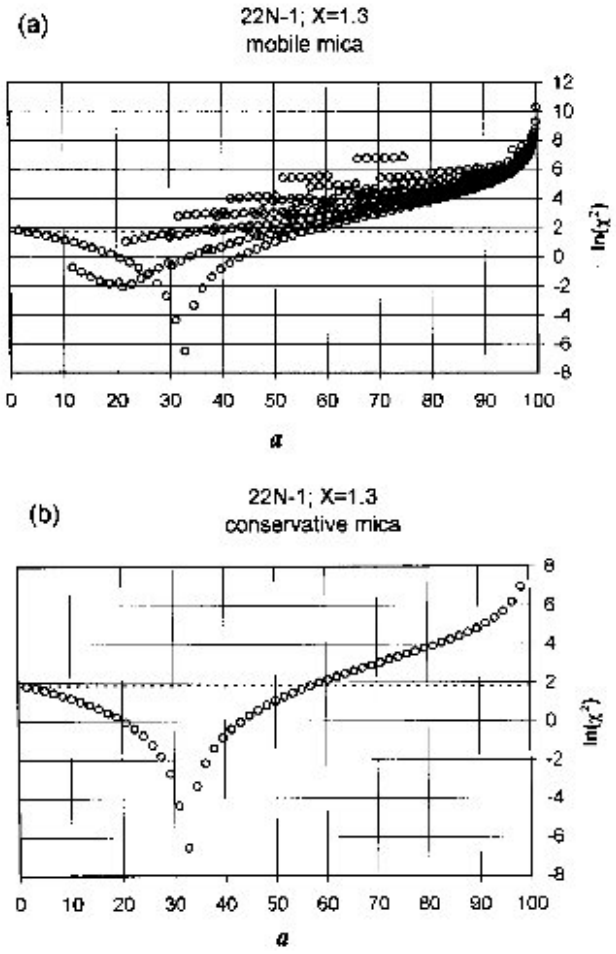

Fig. 6. Results from the chi-square test at 95% significance level ($\alpha = 0.05$, $\chi^2_{2,\alpha} = 5.99$) for the Rohinbera example. See text and Tables 3 and 4 for details. The dashed horizontal line represents the cut-off line at $\alpha = 0.05$, below which overall volume constancy is accepted. (a) Mobile mica model; fold style factor, $X = 1.3$. (b) Conservative mica model; $X = 1.3$. Overall volume constancy is accepted up to a local volume change of $F = 33$, irrespective of the model.

sidered to be associated with best estimates of X in either case.

DISCUSSION AND CONCLUSIONS

Modal analysis using an automatic point counter on thin sections under an optical microscope is a routine petrographic procedure, and can be performed easily, provided the grain size of the rock is in the range resolvable by an optical microscope. Where the rock is a strict two-phase aggregate, image analysis techniques can be adopted for petrographic analysis (e.g. Allard and Sotin, 1988) and one may avoid subjective errors which may creep in while doing modal analysis by point counting.

The test applies best to a situation in which the rock is essentially a two-phase aggregate, i.e. a quartz–mica (muscovite/biotite/chlorite) aggregate with a pre-folding anisotropic but homogeneous fabric. The pre-

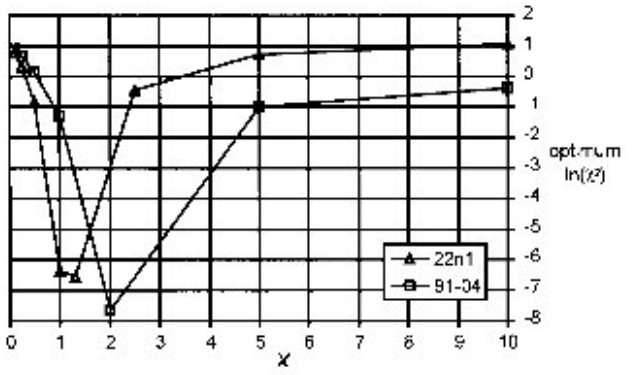

Fig. 7. Dependence of optimum ln (χ^2) on fold style factor, X. The lowest of the optimum ln (χ^2) values corresponds to the best estimate of X (1.33 for the Rohinbera sample, 2.0 for the Galudih sample).

sence of significant amounts of feldspar, calcite or other minerals in addition to quartz that are likely to be 'dissolved' in preference to mica (Heald, 1955; Trurnit, 1968) is likely to complicate the situation. However, one can think of an average quantum of dissolution of 'non-mica' minerals to represent a in the algebraic equations above; during modal analysis the observed mineral counts should accordingly be clubbed together and the test applied.

Mineral redistribution between cleavage domain and microlithon domain during crenulation cleavage development may be significantly modified by concomitant crystallization of mica by metamorphic reactions (Rast, 1966; Weber, 1981) or be grossly modified by later metamorphic overprints. Under such situations the test is inappropriate. Some workers do suggest growth of white mica in low grade (e.g. Knipe, 1981). However, production of mica by metamorphic reactions is volumetrically significant only under higher grades of metamorphism (Gray and Durney, 1979).

A simple test based on the chi-squared statistic and using observed quartz–mica proportions in cleavage and microlithon domains, together with a knowledge of quartz–mica proportions in the original fabric, has been devised to examine whether crenulation cleavage development is an overall volume-constant process or not. Two natural examples of crenulation cleavage from the Singhbhum district, eastern India, were chosen for application of the test. In one, the protolith is marked by a fine homogeneous multilayer fabric with schistosity parallel to layering (Fig. 3d). In the other, it shows a homogeneous schistose fabric. The protolith schistosity becomes crenulated and pressure solution differentiation gives rise to a crenulation cleavage fabric. The mineral association of quartz and white mica with minor amounts of chlorite indicates cleavage development under low grade. In both protoliths, other soluble phases like feldspar and calcite were absent. The texture and microstructure in either example (Figs 3 & 4) suggests selective pressure solution of quartz associated with microfolding and crenulation cleavage development. The examples, there-

fore, satisfy the assumptions for applicability of the test. Application of the test to these examples shows that there are limits to local differential volume loss in the cleavage domains as compared to adjacent microlithon domains, within which the null hypothesis of overall volume constancy is acceptable.

Modal counting is normally associated with statistical error (Kelley, 1971). The plus–minus figures in Table 2 represent 95% confidence limits. For example, in the Galudih sample, there is only a 5% chance that the proportion of quartz is more than 30.65% (28.85 + 1.80) or less than 27.05% (28.85 − 1.80). Thus by changing the input values of Q and M, (quartz and mica proportions in the original fabric) the computations can be repeated in either of the studied examples above for upper and lower bounds of these minerals in the protolith fabric (Table 2) following one or the other end-member models. The expected value of Q and M are then compared with the observed values in the cleavage and microlithon domains of the crenulated fabric, taking into account the statistical errors associated with modal counting in these domains. For example, calculations following the conservative mica model in the Rohinbera sample, taking the upper bound of Q in the different domains (Table 2), show that the global minimum of ln (χ^2) (−8.349) corresponds to an estimate of local volume change, $F = 15\%$ under overall volume constancy, and percentage quartz loss from the cleavage domain, $a = 27.24$; percentage mica loss from microlithon domain, $b = 3.96\%$ at $X = 1.35$. Taking the lower bound of Q in different domains, the best estimate of F is 20%; $a = 35.49\%$; $b = 0$ at $X = 1.2$, under overall volume constancy. Note that the best estimates of F, a, b and X using mean quartz and mica proportions lie between those corresponding to lower and upper bounds of mineral proportions, respectively, and those mentioned above. Evidently, the null hypothesis of overall volume constancy is accepted in either of the examples, even taking into account the statistical errors associated with modal counting. The global minimum of ln (χ^2) and the corresponding estimates of local volume changes are quite close to those in Tables 3 and 4.

The global minimum of the χ^2 statistic is associated with a zero value of b, the proportion of mica (expressed as %) removed from the microlithons; therefore, the conservative mica model of mineral redistribution for cleavage differentiation is apparently more appropriate in the examples cited above than the mobile mica model. However, at a significance level of $\alpha = 0.05$, overall volume constancy cannot be rejected for a small but non-zero b and X in the range from 0.1 to 10 ($X = 2$ for Galudih and $X = 1.3$ for Rohinbera leads to zero b). Thus the mobile mica model of mineral redistribution cannot be rejected altogether. The numerical exercise, however, demonstrates that mica is definitely much less mobile compared to quartz during crenulation cleavage differentiation.

Acknowledgements—My sincere thanks to John Cosgrove, Neil S. Mancktelow and Richard J. Lisle for improvements on an earlier version of the manuscript. Constructive criticisms from David Anastasio and David Gray who reviewed the manuscript and additional comments from Peter Hudleston are gratefully acknowledged. Ajoy Das drafted Fig. 1. Research for this work is supported by Indian Statistical Institute, Calcutta.

REFERENCES

Alvarez, W., Engelder, T. and Geiser, P. A. (1978) Classification of solution cleavage in pelagic limestones. *Geology* **6,** 263–266.

Allard, B. and Sotin, C. (1988) Determination of mineral phase percentages in granular rocks by image analysis on a microcomputer. *Computers and Geosciences* **14,** 261–269.

Beach, A. (1979) Pressure solution as a metamorphic process in deformed terrigenous sedimentary rocks. *Lithos* **12,** 51–58.

Berensen, M. L., Levine, D. M. and Goldstein, M. (1982) *Intermediate Statistical Methods and Applications*. Prentice-Hall, Englewood Cliffs, New Jersey.

Borradaile, G. J., Bayly, M. B. and Powell, C. McA. (1982) *Atlas of Deformational and Metamorphic Rock Fabrics*. Springer, Berlin.

Caron, J. M., Potdvein, J. L. and Sicard, E. (1987) Solution-deposition processes and mass transfer in the deformation of a minor fold. *Tectonophysics* **135,** 77–86.

Cheeney, R. F. (1983) *Statistical Methods for Geologists*. George Allen Unwin, London.

Cosgrove, J. W. (1976) The formation of crenulation cleavage. *Journal of the Geological Society London* **132,** 155–178.

Dunn, J. A. and Dey, A. K. (1942) *The Geology and Petrology of Eastern Singhbhum and Surrounding Areas*. Geological Survey of India Memoir.

Durney, D. W. (1972) Solution-transfer, an important geological deformation mechanism. *Nature* **235,** 315–317.

Elliott, D. (1973) Diffusional flow laws in metamorphic rocks. *Geological Society of America Bulletin* **84,** 2645–2664.

Etheridge, M. A., Wall, V. J., Cox, S. F. and Vernon, R. H. (1984) High fluid pressures during regional metamorphism and deformation: implication for mass transport and deformation mechanisms. *Journal Geophysical Research* **89,** 4344–4358.

Galehouse, J. S. (1971) Point Counting. In *Procedures in Sedimentary Petrology*, ed. R. E. Carver, pp. 385–407. Wiley-Interscience, New York.

Granath, J. W. (1980) Strain, metamorphism, and the development of differentiated crenulation cleavages at Cooma, Australia. *Journal of Geology* **88,** 589–601.

Gray, D. R. (1977a) Morphologic classification of crenulation cleavage. *Journal of Geology* **85,** 229–235.

Gray, D. R. (1977b) Some parameters which affect the morphology of crenulation cleavages. *Journal of Geology* **85,** 763–780.

Gray, D. R. (1979) Microstructure of crenulation cleavages: an indicator of cleavage origin. *American Journal of Science* **279,** 97–128.

Gray, D. R. and Durney, D. W. (1979) Crenulation cleavage differentiation: implications of solution-deposition processes. *Journal of Structural Geology* **1,** 73–80.

Heald, M. T. (1955) Stylolites in sandstones. *Journal of Geology* **63,** 101–114.

Hobbs, B. E., Means, W. D. and Williams, P. F. (1976) *Outline of Structural Geology*. John Wiley and Sons, New York.

Kelley, J. C. (1971) Mathematical analysis of point count data. In *Procedures in Sedimentary Petrology*, ed. R. E. Carver, pp. 407–425. Wiley-Interscience, New York.

Knipe, R. J. (1981) The interaction of deformation and metamorphism in slates. *Tectonophysics* **78,** 249–272.

Knipe, R. J. and White, S. H. (1977) Microstructural variation of an axial plane cleavage around a fold—a H. V. E. M study. *Tectonophysics* **39,** 355–380.

Mancktelow, N. S. (1994) On volume change and mass transport during development of crenulation cleavage. *Journal of Structural Geology* **16,** 1217–1231.

Marlow, P. C. and Etheridge, M. A. (1977) The development of a layered crenulation cleavage in mica-schists of the Kanmantoo Group near Macclesfield, South Australia. *Geological Society of America Bulletin* **88,** 873–882.

Powell, C. McA. (1979) A morphologic classification of rock cleavage. *Tectonophysics* **58,** 21–34.

Price, N. J. and Cosgrove, J. W. (1990) *Analysis of Geological Structures*. Cambridge University Press, Cambridge.

Rast, N. (1965) Nucleation and growth of metamorphic minerals. In *Controls of Metamorphism*, ed. W. S. Pitcher and G. W. Flinn, pp. 73–102. John Wiley, New York.

Rutter, E. H. (1976) The kinetics of rock deformation by pressure solution. *Philosophical Transactions Royal Society London* **A283,** 203–219.

Rutter, E. H. (1983) Pressure solution in nature, theory and experiment. *Journal of the Geological Society London* **140,** 725–740.

Saha, D. (1995) Some observations on brittle–ductile toggle. *Proceedings of the Indian Academy of Sciences (Earth and Planetary Sciences)* **104,** 419–431.

Sarkar, A. N. (1982) Precambrian tectonic evolution of Eastern India: a model of converging microplates. *Tectonophysics* **86,** 363–397.

Sarkar, S. N. and Saha, A. K. (1977) The present status of Precambrian stratigraphy, tectonics and geochronology of Singhbhum–Keonjhar–Mayurbhanj region, eastern India. *Indian Journal Earth Science* (S. Ray volume), 37–65.

Trurnit, P. (1968) Pressure solution phenomena in detrital rocks. *Sedimentary Geology* **2**, 89–114.

Weber, K. (1981) Kinematic and metamorphic aspects of cleavage formation in very low grade metamorphic slates. *Tectonophysics* **78,** 291–306.

Wintsch, R. P., Kvale, C. M. and Kisch, H. J. (1991) Open-system, constant-volume development of slaty cleavage, and strain-induced replacement reactions in the Martinsburg Formation, Lehigh Gap, Pennsylvania. *Geological Society of America Bulletin* **103,** 916–927.